La Compacidad Discreta y sus Aplicaciones

por Ernesto Bribiesca

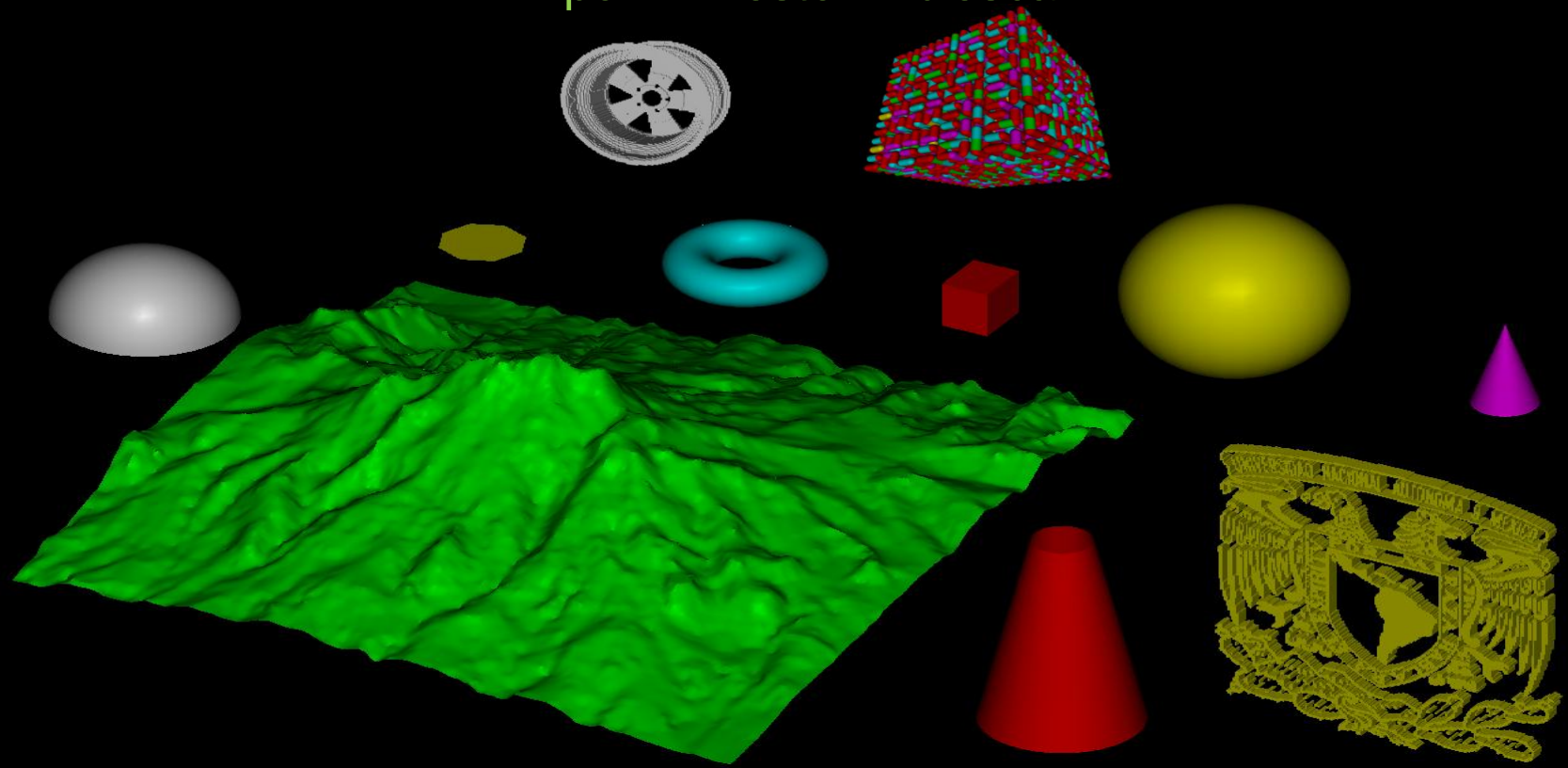

$C=P^2/A$

La Compacidad Clásica

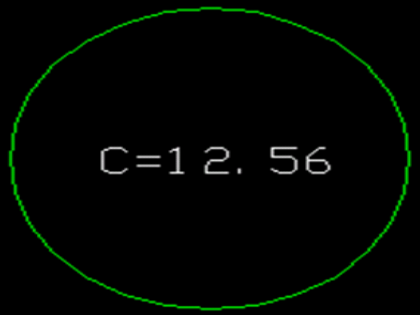

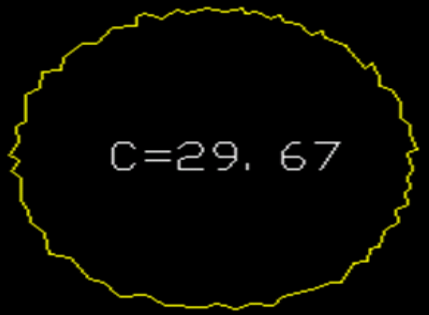

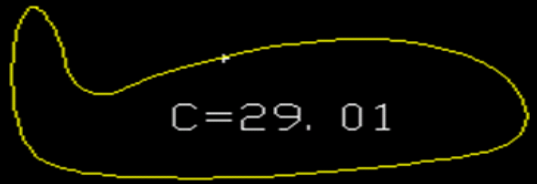

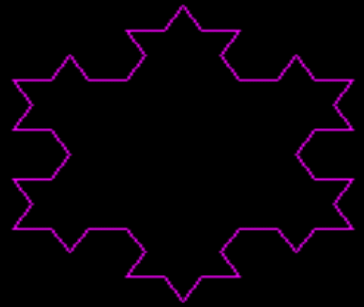

Perímetro de Contacto

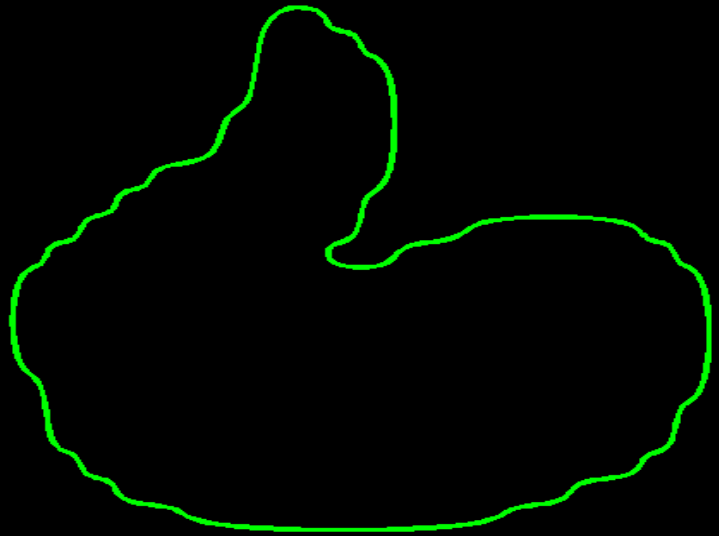

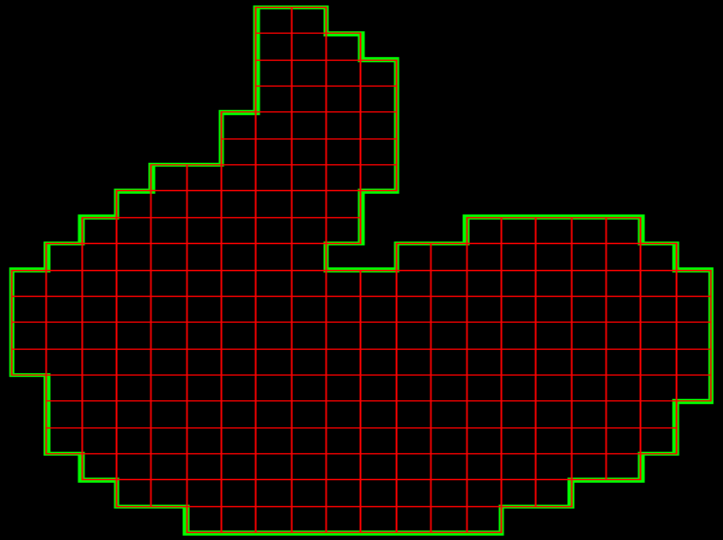

Perímetro de Contacto

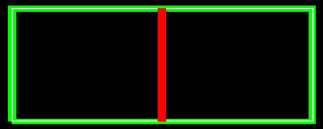

$$P + 2P_c = 4n$$

Donde:

P es el perimetro
P_c es el perimetro de contacto
n es el número de pixels

$$6 + 2(1) = 4(2)$$

Compacidad Discreta Normalizada con valores del cero al uno

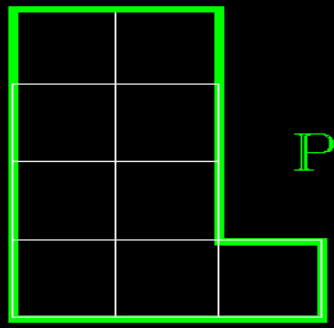

$$P + 2P_c = 4n$$

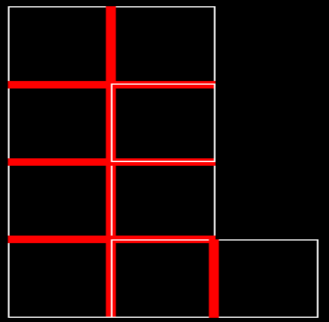

$$C_D = \frac{P_c}{P_{c\,max}}$$

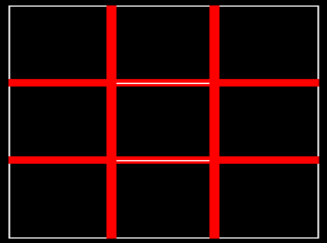

$$P_{c\,max} = \frac{4n - 4\sqrt{n}}{2}$$

$$P_{c\,max} = 2(n - \sqrt{n})$$

$$C_d = \frac{n - P/4}{n - \sqrt{n}}.$$

La Compacidad Clásica en tres dimensiones es igual a la superficie al cubo entre el volumen al cuadrado

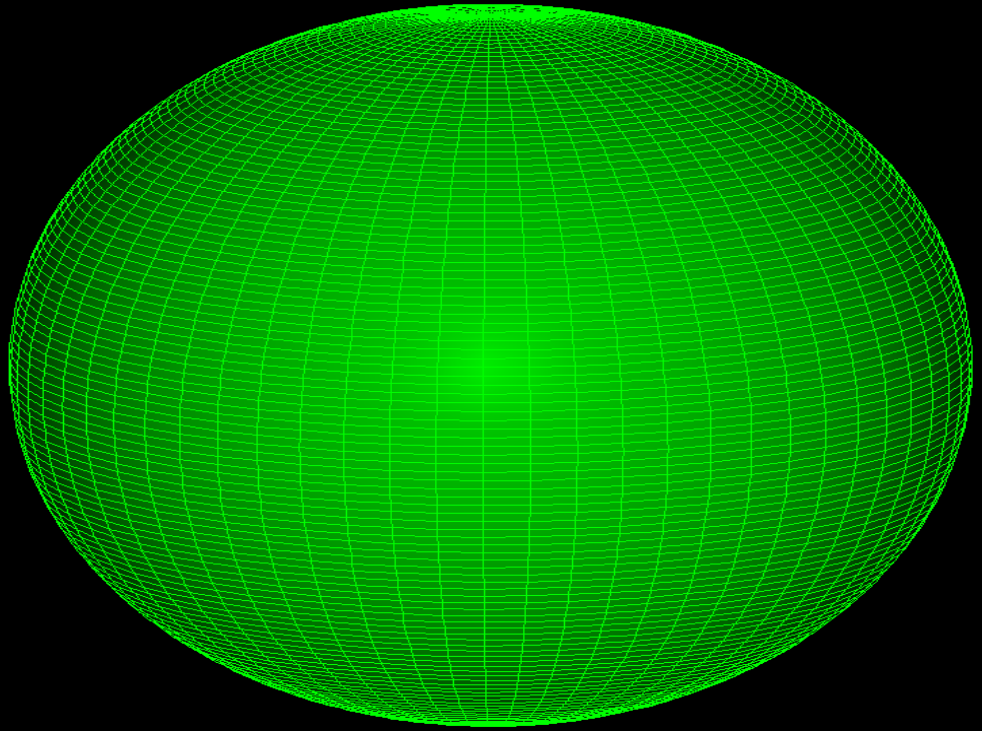

C=113.0973

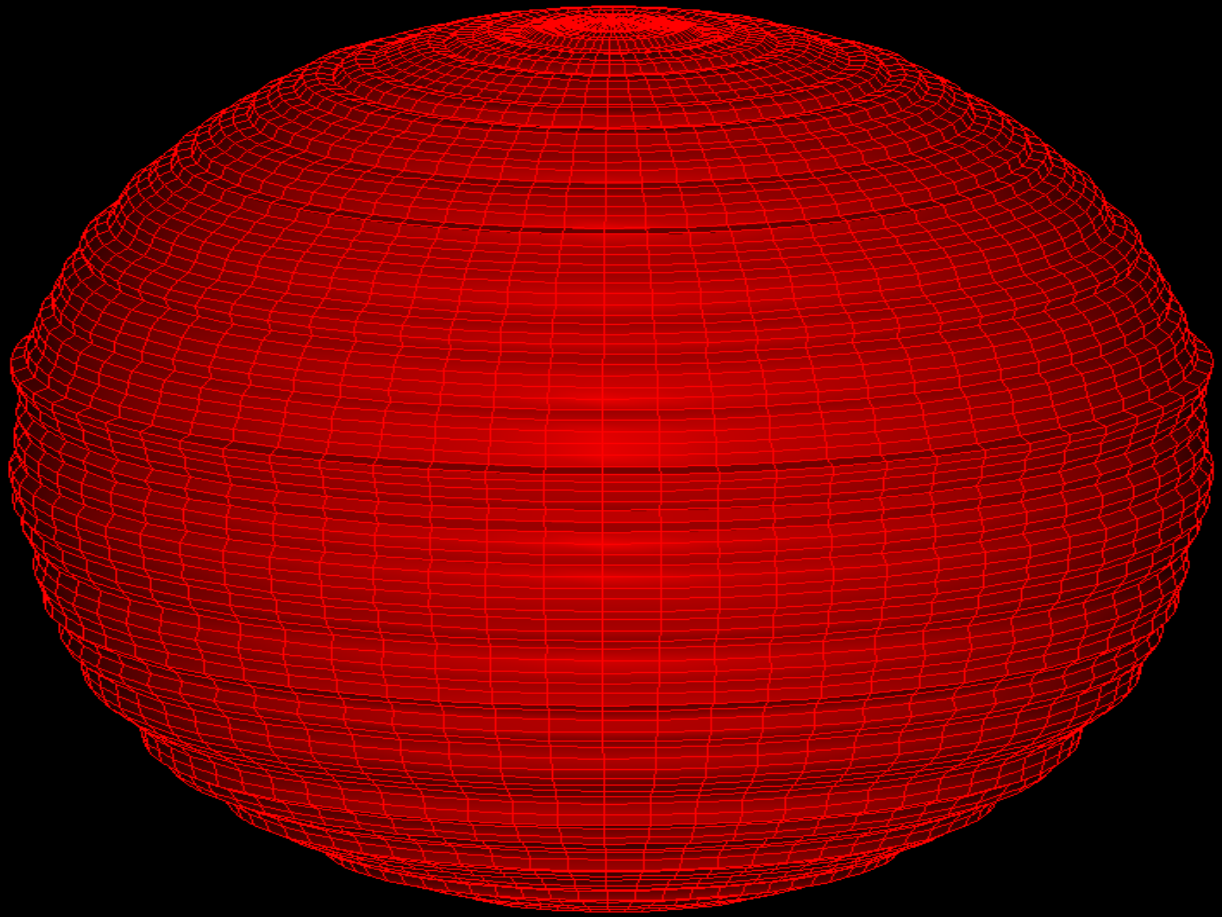
C=159.8176

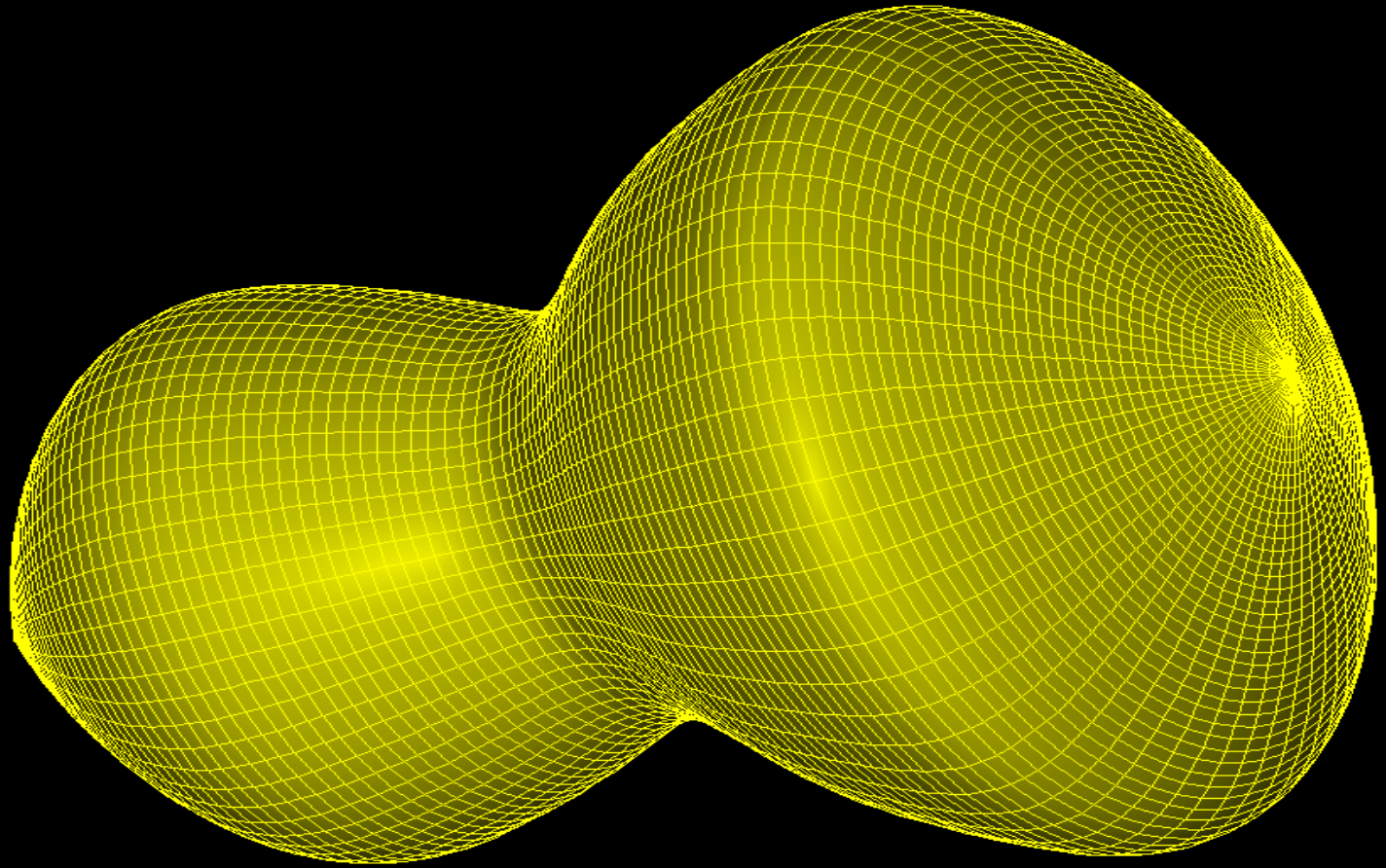
C=123.4025

La Compacidad Discreta

$$C_d = \frac{n - A/6}{n - (\sqrt[3]{n})^2}.$$

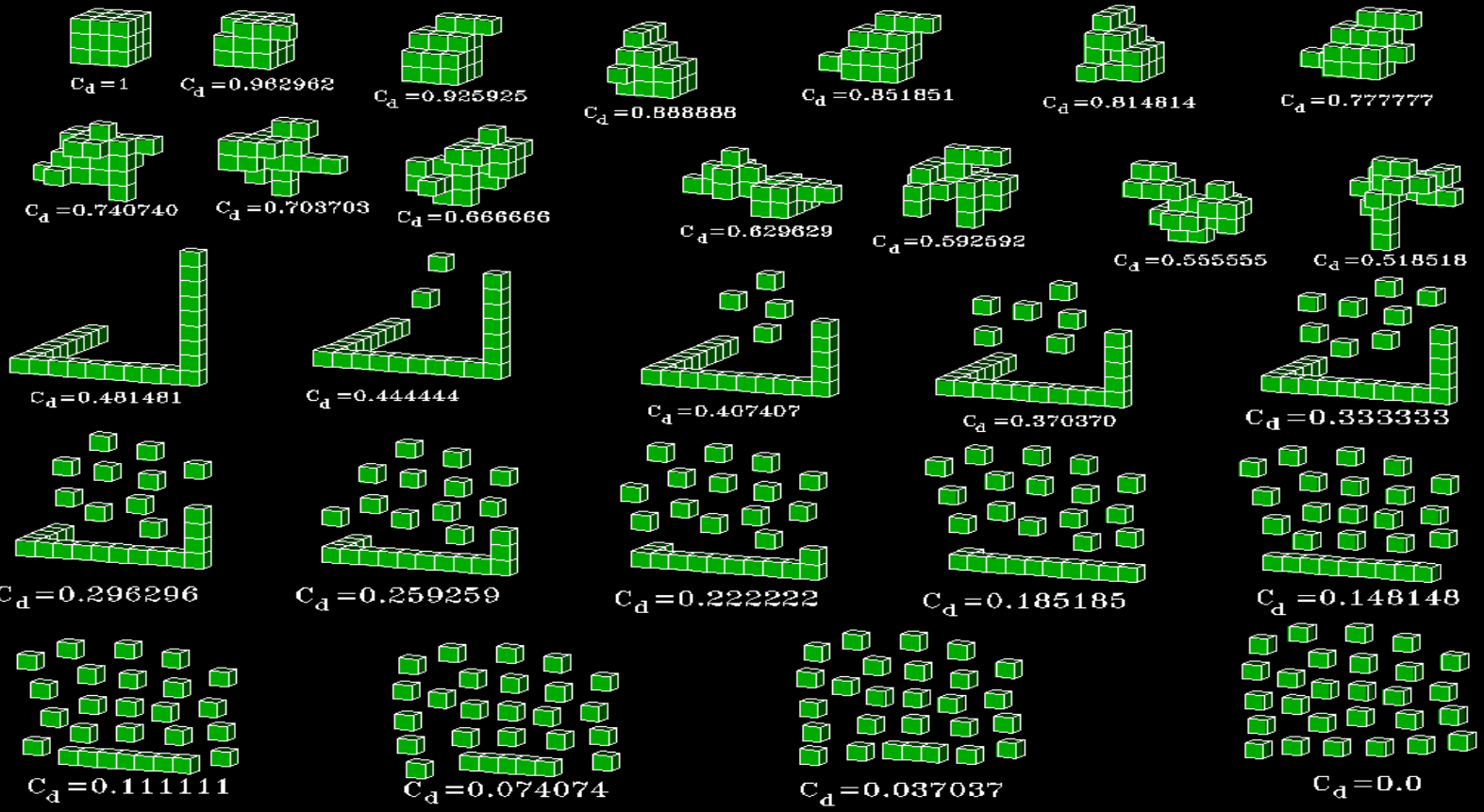

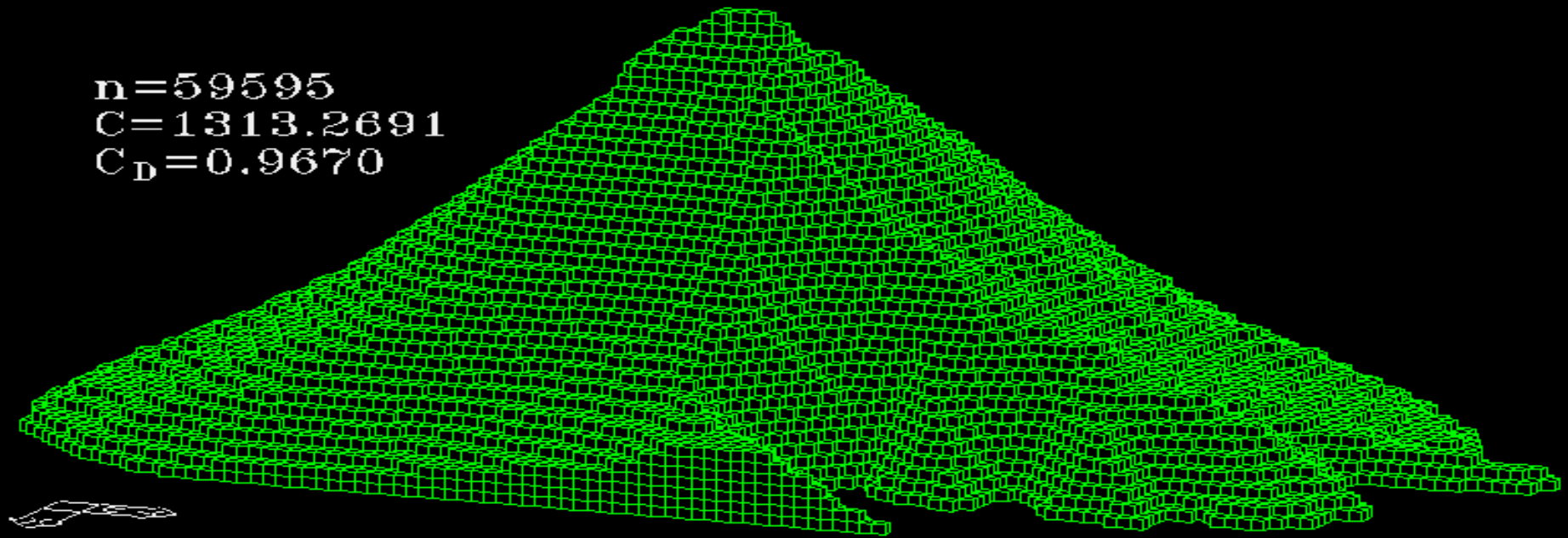
n=59595
C=1313.2691
C_D=0.9670

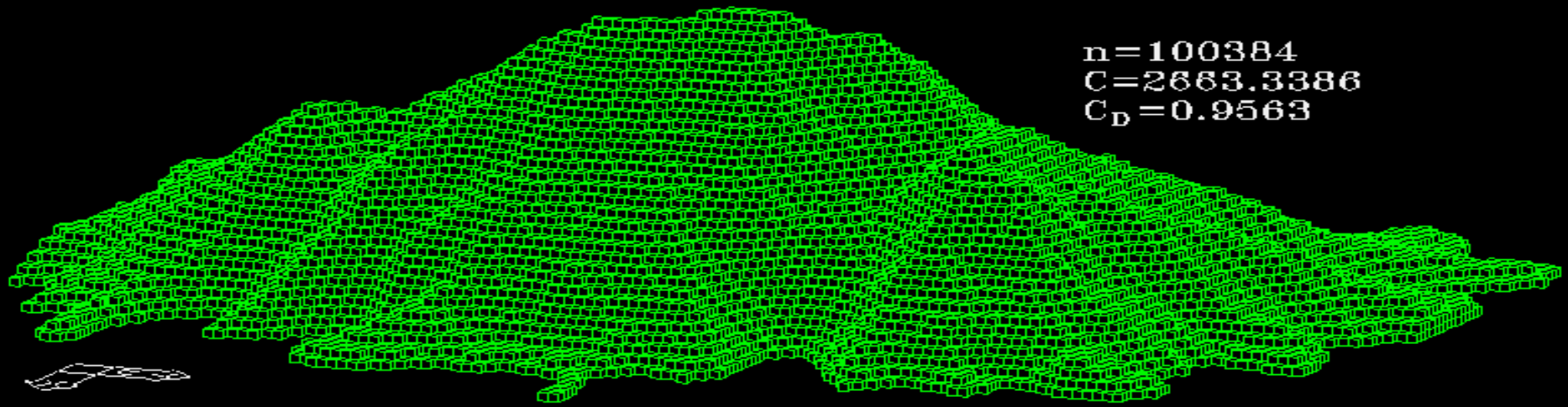
n=100384
C=2663.3386
C_D=0.9563

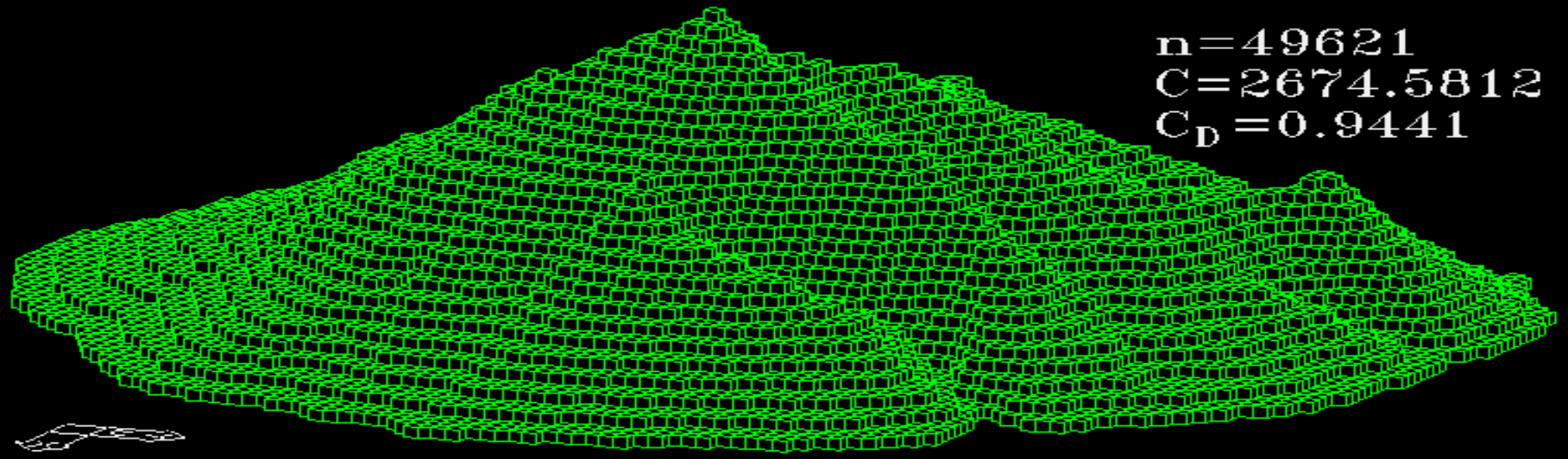
n=49621
C=2674.5812
C_D=0.9441

Three-Dimensional Reconstruction and Quantification of Cervical Carcinoma Invasion Fronts From Histological Serial Sections

Ulf-Dietrich Braumann, *Member, IEEE*, Jens-Peer Kuska, *Member, IEEE*, Jens Einenkel, Lars-Christian Horn, Markus Löffler, and Michael Höckel

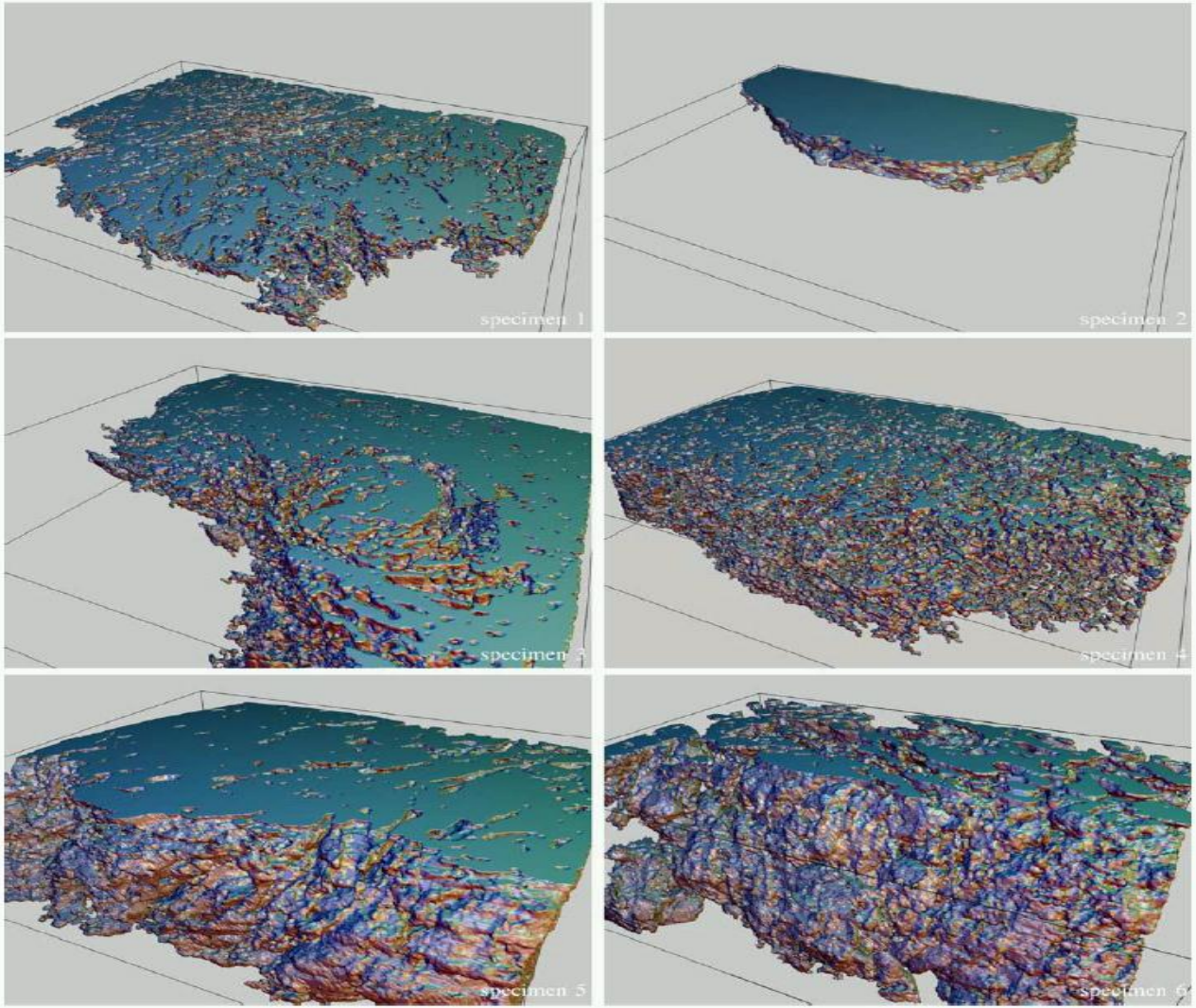
specimen 1
specimen 2
specimen 5

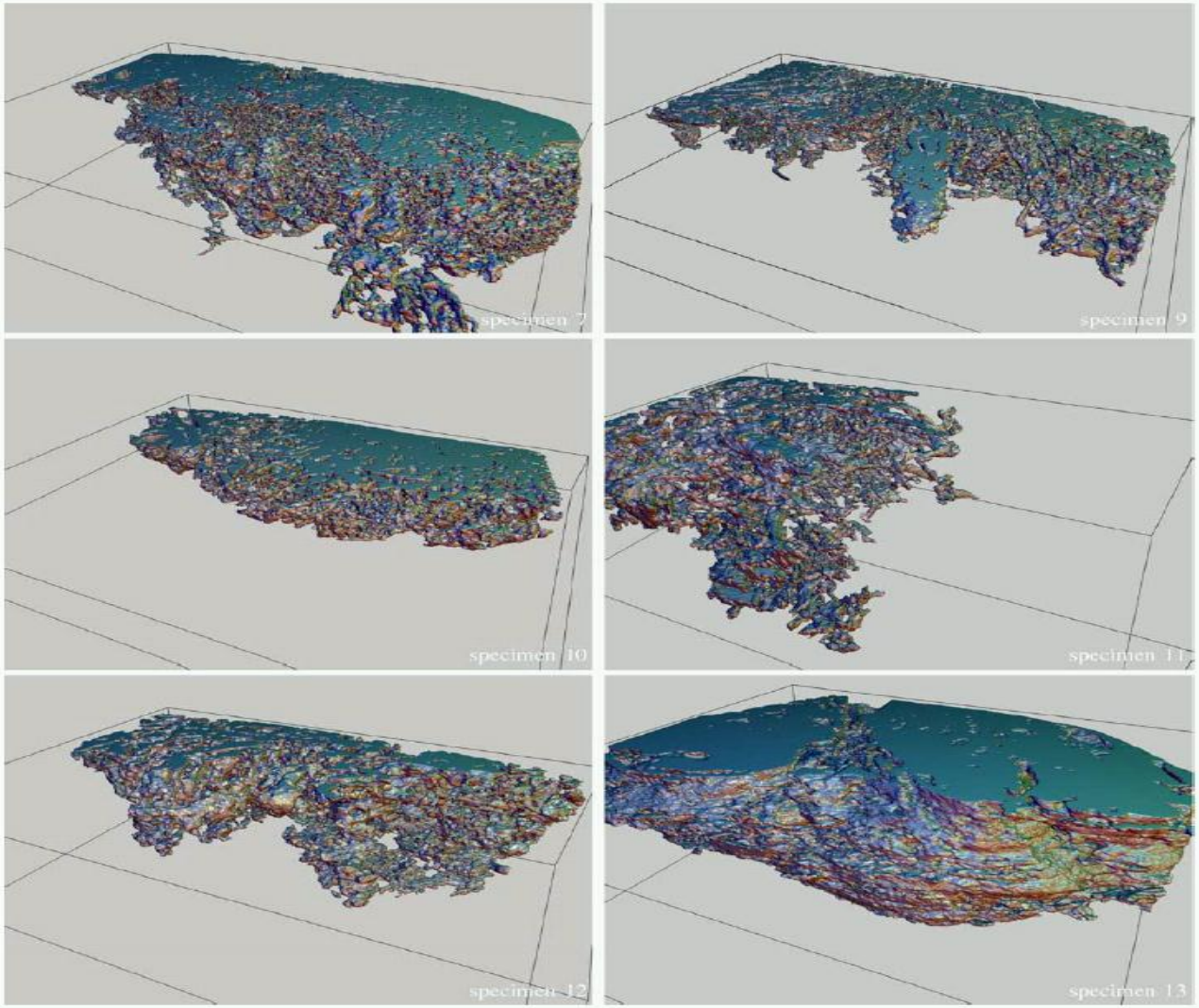
specimen 7
specimen 9
specimen 10
specimen 11
specimen 12
specimen 13

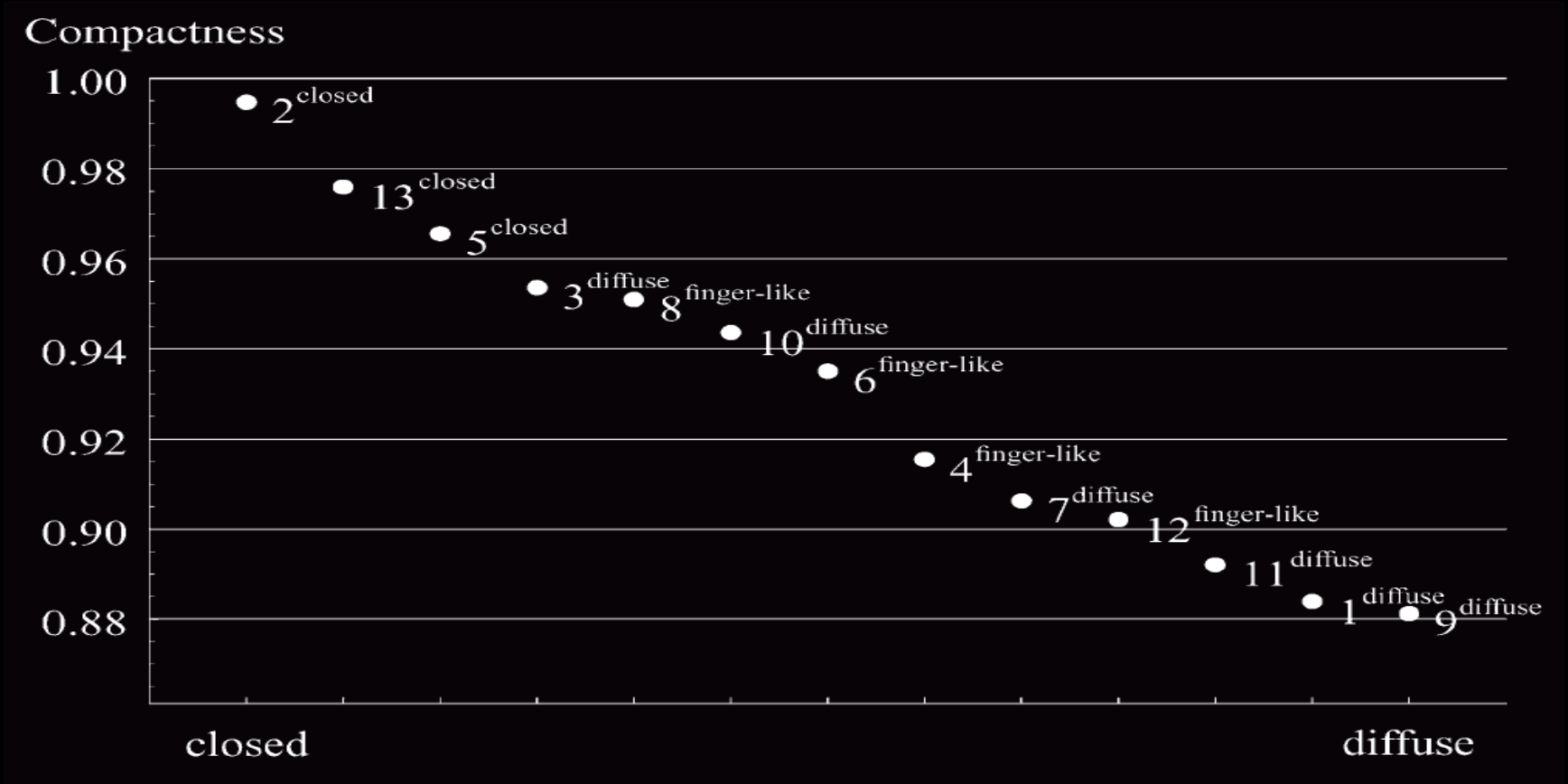
Compactness
1.00
0.98
0.96
0.94
0.92
0.90
0.88
2 closed
13 closed
5 closed
3 diffuse
8 finger-like
10 diffuse
6 finger-like
4 finger-like
7 diffuse
12 finger-like
11 diffuse
1 diffuse
9 diffuse
closed
diffuse

Proceedings of the 29th Annual International
Conference of the IEEE EMBS
Cité Internationale, Lyon, France
August 23-26, 2007.

Shape Characterization of Extracted and Simulated Tumor Samples using Topological and Geometric Measures

Markus Rohrschneider*, Gerik Scheuermann*, Stefan Hoehme†, Dirk Drasdo‡

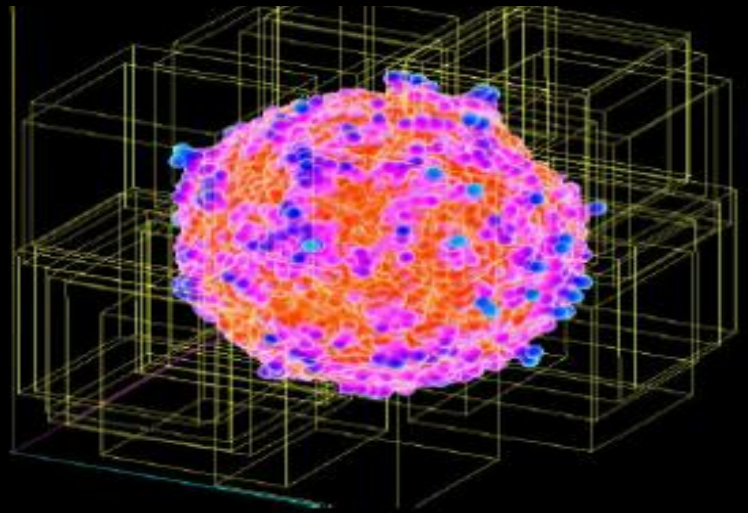

Fig. 2. Boundary of simulated tumor sample id120_mot1. The bounding boxes of 30 random samples are shown.

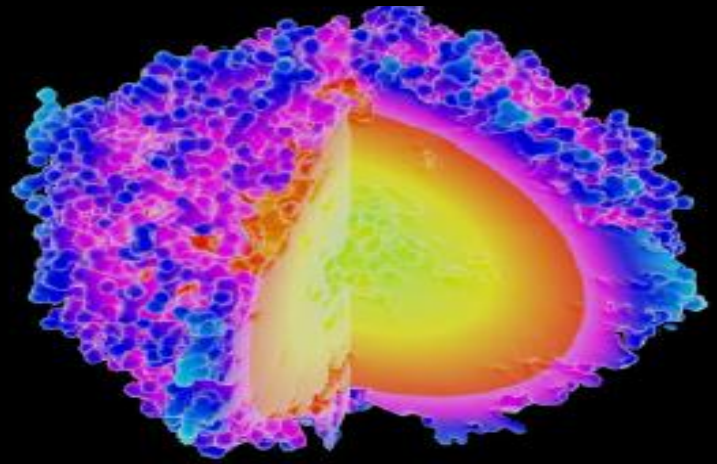

Fig. 3. Boundary of simulated tumor sample id100_mot30. The inner surface due to the necrotic core is shown.

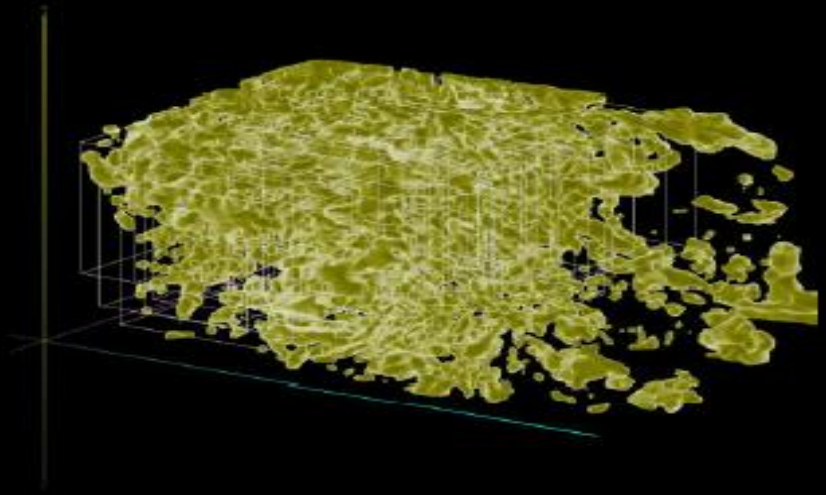

Fig. 6. Boundary of cervix carcinoma specimen 11 (diffuse tumor type). The bounding boxes of 30 random samples containing approx. 13% foreground voxels, are shown.

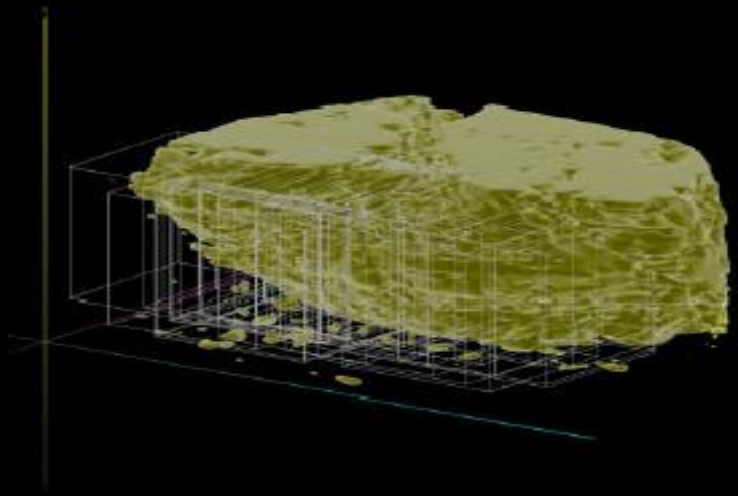

Fig. 7. Boundary of cervix carcinoma specimen 13 (compact tumor type). The bounding boxes of 30 random samples containing approx. 27% foreground voxels, are shown. The object contains many small cavities not visible in this representation.

TABLE I

RESULTS OF THE COMPACTNESS COMPUTATION AND TOPOLOGICAL ANALYSIS.

Dataset	Average of 30 Samples							Complete Object				
	Area	Volume	Compactness		β_0	β_1	β_2	Compactness		β_0	β_1	β_2
1. asym_mot1	15618.5	198596	0.85	0.9876	1.00	11.01	0.00	6.67	0.9929	1	176	0
2. asym_mot20	28815.9	192697	5.70	0.9717	1.07	33.03	0.00	60.41	0.9773	2	624	0
3. id095_mot1	27406.1	199477	4.57	0.9750	1.43	40.08	0.00	36.86	0.9809	6	468	0
4. id100_mot1	24598.7	190235	3.64	0.9766	1.33	35.39	0.00	28.55	0.9835	5	475	0
5. id100_mot10	33698.5	189090	9.46	0.9662	1.37	43.27	0.00	74.92	0.9723	5	475	0
6. id100_mot20	34658.0	185317	10.72	0.9647	1.07	40.03	0.00	100.39	0.9688	2	447	0
7. id100_mot30	46132.2	184418	25.53	0.9507	1.00	288.88	1.59	254.65	0.9564	1	2867	17
8. id100_mot1_adh	32872.8	195883	8.19	0.9680	1.03	101.50	0.00	66.16	0.9768	2	1301	0
9. id120_mot1	18581.0	200296	1.41	0.9844	1.00	24.27	0.00	10.76	0.9903	1	316	0
10. cerv11 (diffuse type)	89644.6	134022	354.66	0.8800	110.43	101.11	0.75	3337.46	0.8742	934	618	5
11. cerv13 (compact type)	55138.9	273947	19.75	0.9601	50.37	106.11	36.41	114.21	0.9758	334	1284	755

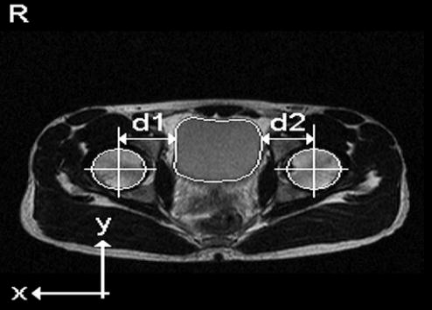

(b)

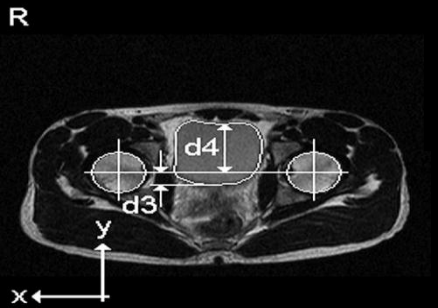

(c)

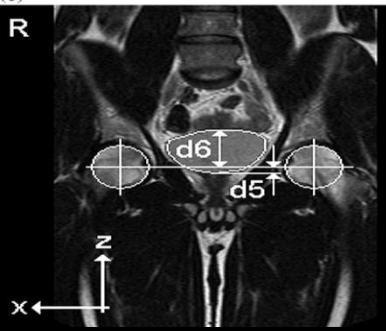

ORIGINAL ARTICLE

Taylor & Francis healthsciences

Effect of Bladder Volume, Gender and Body Position on the Shape and Position of the Urinary Bladder

Niels Kristian Kristiansen,[1,2] Steffen Ringgaard,[3] Hans Nygaard[2,4] and Jens Christian Djurhuus[1]

From the [1]Clinical Institute, Aarhus University Hospital, Skejby Sygehus, Aarhus, Denmark, [2]Department of Electronics and Information Technology, University College of Aarhus, Aarhus, Denmark and the [3]MR-Center and [4]Department of Cardiothoracic & Vascular Surgery, Aarhus University Hospital, Skejby Sygehus, Aarhus, Denmark

(Submitted December 15, 2003. Accepted for publication May 19, 2004)

Scand J Urol Nephrol 38: 462–468, 2004

Ultrasound in Med. & Biol., Vol. 37, No. 4, pp. 539–548, 2011

0301-5629/$ - see front matter

ELSEVIER

doi:10.1016/j.ultrasmedbio.2011.01.006

Original Contribution

COMPUTER-AIDED DIAGNOSIS FOR THE CLASSIFICATION OF BREAST MASSES IN AUTOMATED WHOLE BREAST ULTRASOUND IMAGES

Woo Kyung Moon,* Yi-Wei Shen,† Chiun-Sheng Huang,‡ Li-Ren Chiang,† and Ruey-Feng Chang†§

*Department of Diagnostic Radiology, Seoul National University Hospital, Korea; †Department of Computer Science and Information Engineering, National Taiwan University, Taipei, Taiwan; ‡Department of Surgery, National Taiwan University Hospital, Taipei, Taiwan; and §Graduate Institute of Biomedical Electronics and Bioinformatics, National Taiwan University, Taipei, Taiwan

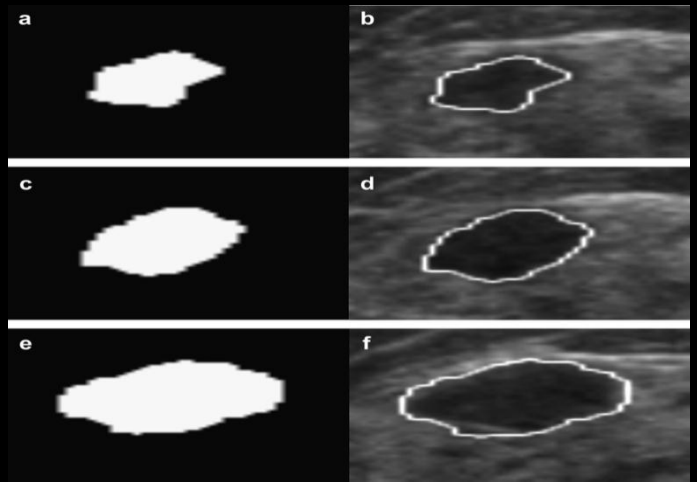

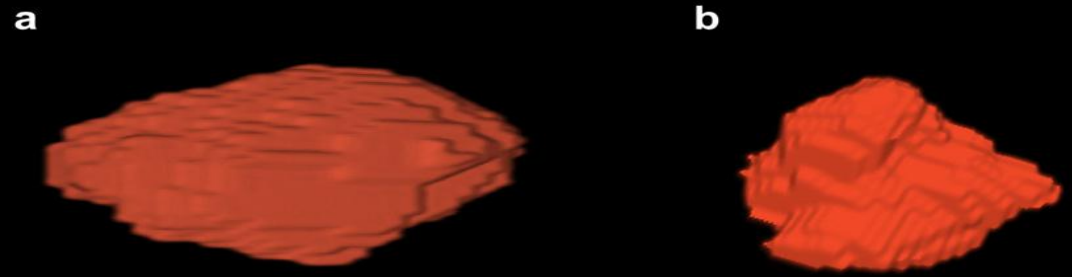

International Journal of Remote Sensing
Vol. 30, No. 24, 20 December 2009, 6621–6628

Taylor & Francis
Taylor & Francis Group

Remote Sensing Letters

Characterization of individual tree crowns using three-dimensional shape signatures derived from LiDAR data

PINLIANG DONG*
Department of Geography, University of North Texas, Denton, TX 76203, USA

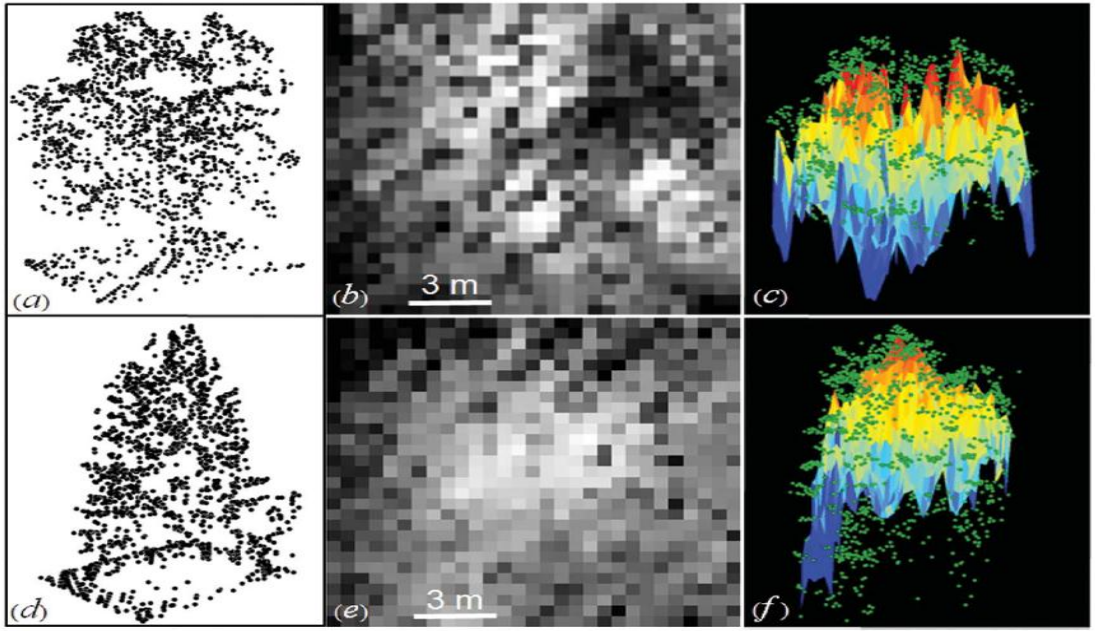

Figure 2. LiDAR data point cloud perspective views, DSM, and combined perspective display of point clouds and DSM. Top row: oak; bottom row: Douglas fir.

Ecological Modelling 221 (2010) 433–444

Contents lists available at ScienceDirect

Ecological Modelling

journal homepage: www.elsevier.com/locate/ecolmodel

Deriving state-and-transition models from an image series of grassland pattern dynamics

Rohan J. Sadler[a,b,c,*], Martin Hazelton[d], Matthias M. Boer[a,c], Pauline F. Grierson[a,c]

[a] Ecosystems Research Group, School of Plant Biology, The University of Western Australia, 35 Stirling Highway, Crawley, 6009, Australia
[b] School of Mathematics and Statistics, The University of Western Australia, 35 Stirling Highway, Crawley, 6009, Australia
[c] Bushfire Cooperative Research Centre, Level 5, 340 Alberty Street, East Melbourne, VIC 3002, Australia
[d] Institute of Information Sciences and Technology, Massey University, Private Bag 11 222, Palmerston North, New Zealand

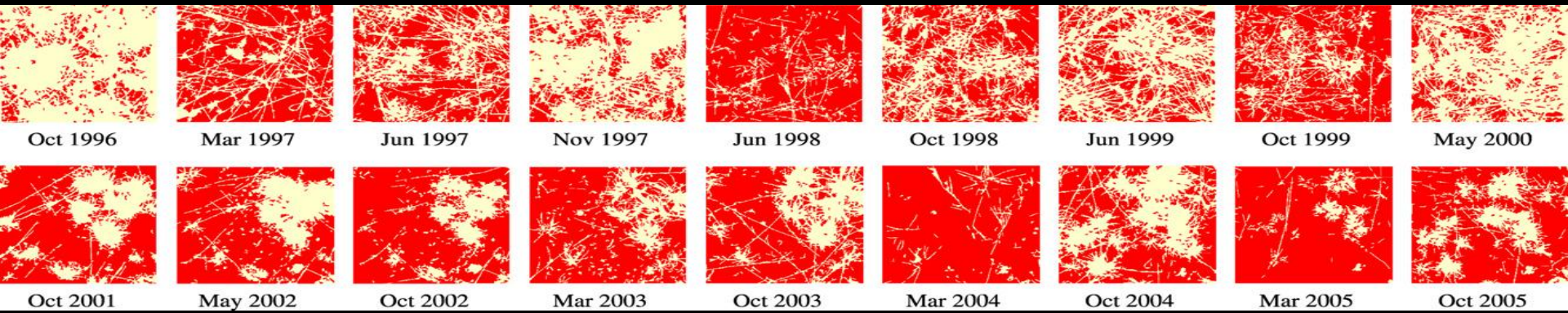

Contents lists available at SciVerse ScienceDirect

Computer-Aided Design

journal homepage: www.elsevier.com/locate/cad

A real-time assessment of the ship design complexity

J.-D. Caprace *, P. Rigo

ANAST – University of Liège, Chemin des chevreuils, 1, 4000 Liège, Belgium

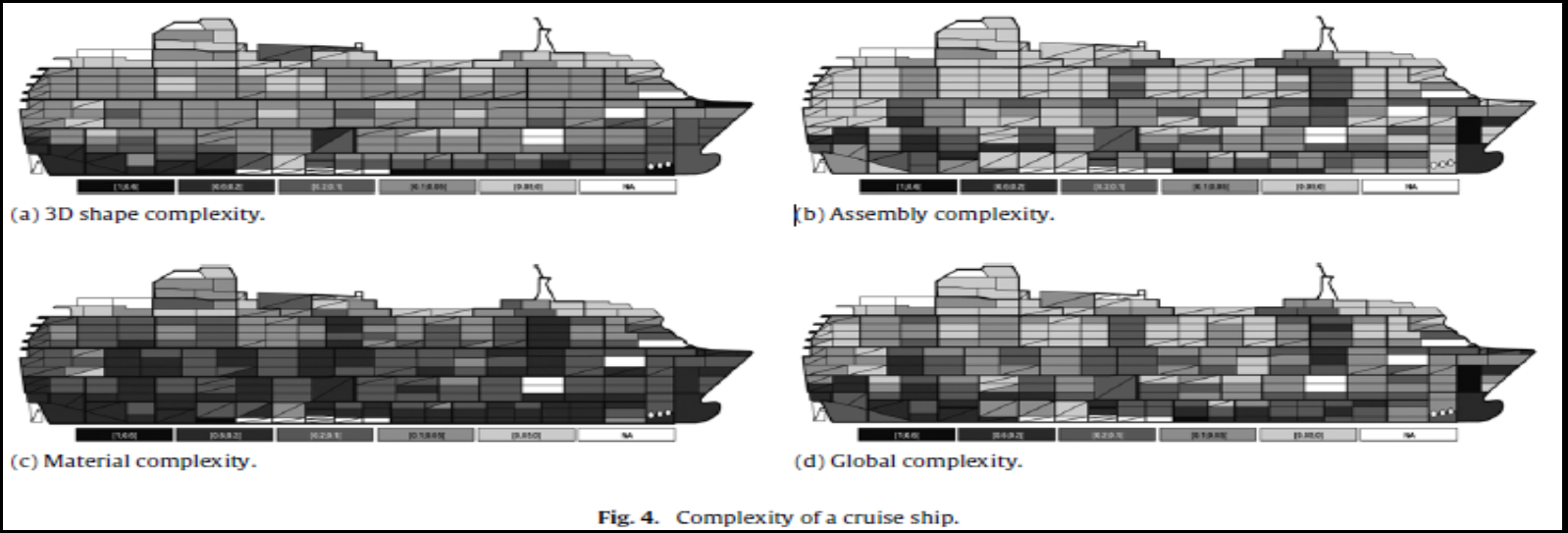

(a) 3D shape complexity.

(b) Assembly complexity.

(c) Material complexity.

(d) Global complexity.

Fig. 4. Complexity of a cruise ship.

IOP PUBLISHING PHYSICS IN MEDICINE AND BIOLOGY
Phys. Med. Biol. 54 (2009) 7009–7024 doi:10.1088/0031-9155/54/22/017

Airway segmentation and analysis for the study of mouse models of lung disease using micro-CT

X Artaechevarria[1], D Pérez-Martín[1], M Ceresa[1], G de Biurrun[2], D Blanco[2], L M Montuenga[2], B van Ginneken[3], C Ortiz-de-Solorzano[1] and A Muñoz-Barrutia[1]

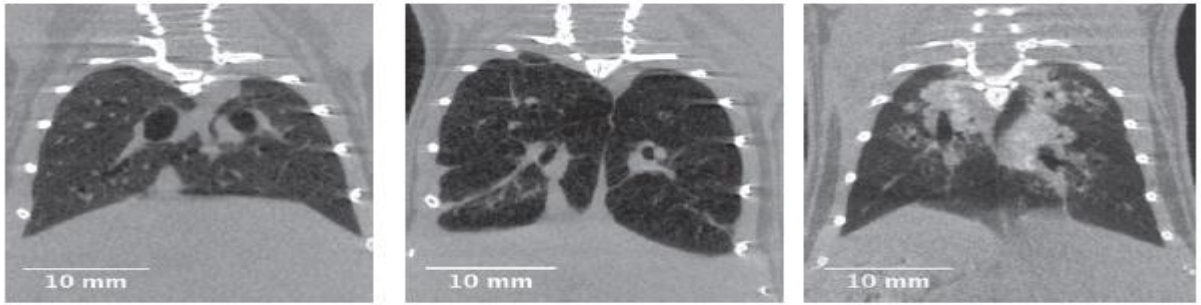

(a) Control (b) Emphysema (c) Inflammation

Figure 2. Sample coronal micro-CT slices of control, emphysematous and inflammed mice lungs. Differences in lung texture and shape are clearly visible.

Then, the discrete compactness (C) is computed, as defined by Bribiesca (2008) for a solid volume of n voxels in 3D:

$$C = \frac{n - A/6}{n - (\sqrt[3]{n})^2}, \tag{4}$$

Image Processing Methods for Automatic Cell Counting In Vivo or In Situ Using 3D Confocal Microscopy

Manuel G. Forero[1] and Alicia Hidalgo[2]
[1]*Cardiff University,*
[2]*University of Birmingham,*
United Kingdom

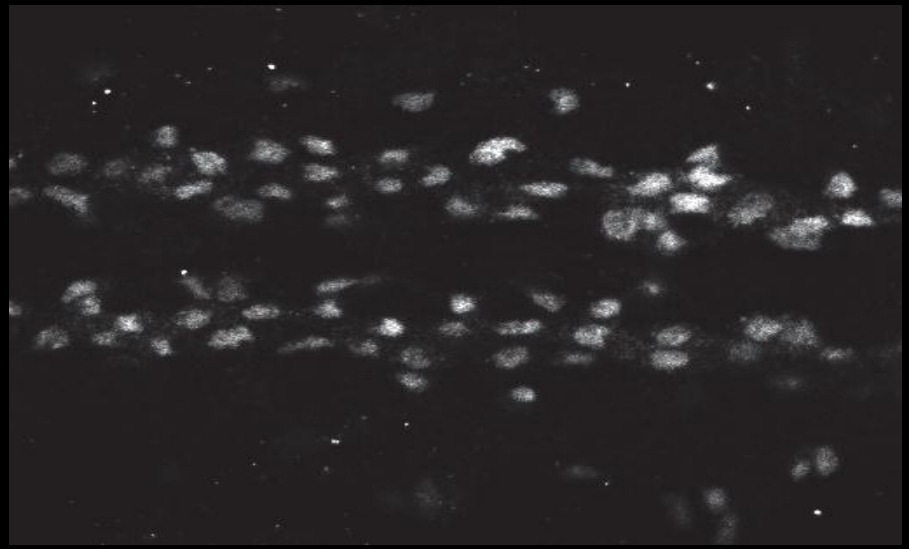

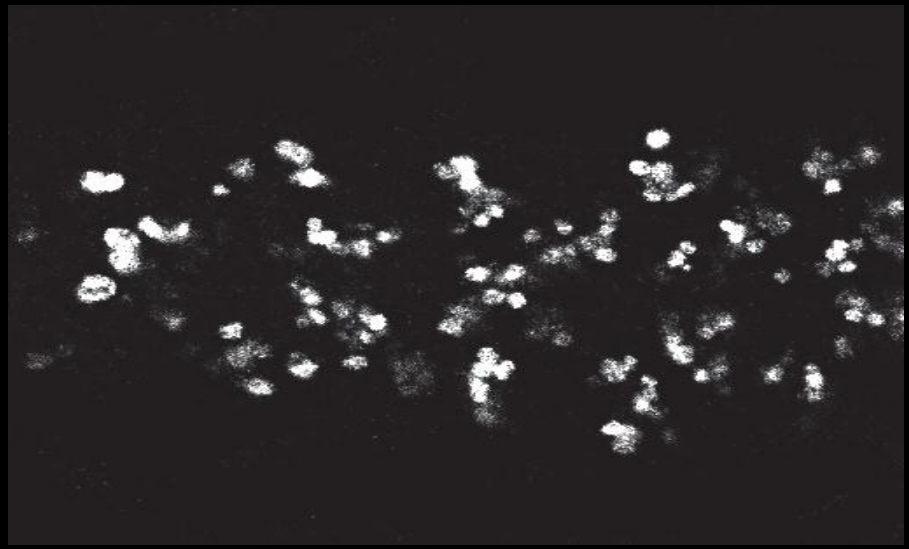

Compacidad en celdas aplicada al diseño de zonas electorales

ERIC RINCÓN GARCÍA
MIGUEL ANGEL GUTIÉRREZ ANDRADE [1]

Zonas generadas al aplicar la compacidad por celdas

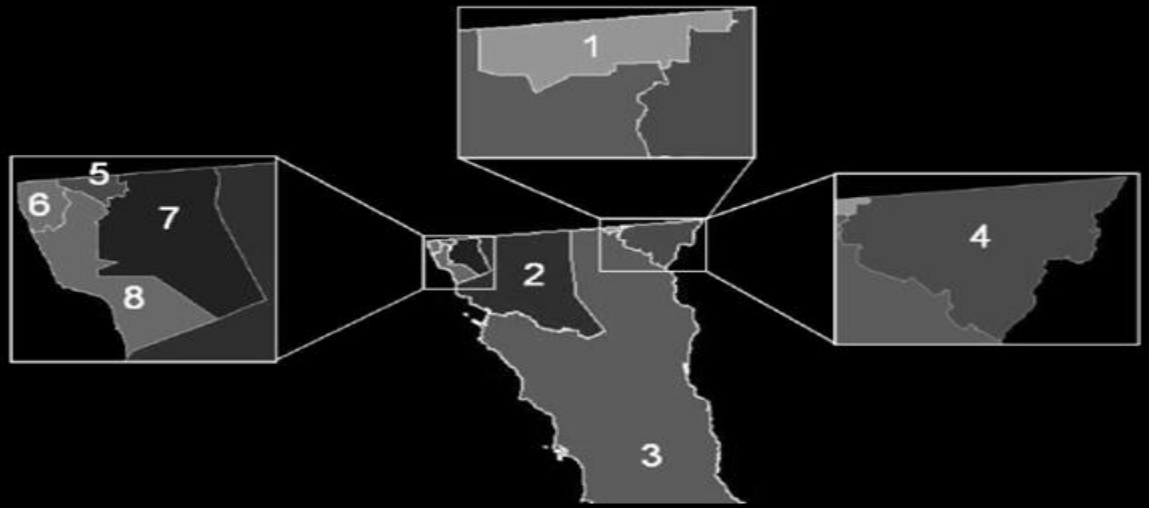

Spatial Dispersion of Lesions as a Surrogate Biomarker for Disability in Multiple Sclerosis

Fahime Sheikhzadeh
MS/MRI Research Group
University of British Columbia
Vancouver, BC, Canada, V6T 1Z4
fahime@msmri.medicine.ubc.ca

Roger Tam
MS/MRI Research Group
University of British Columbia
Vancouver, BC, Canada, V6T 1Z4
roger.tam@ubc.ca

Ghassan Hamarneh
Medical Image Analysis Lab
Simon Fraser University
Vancouver, BC, Canada, V5A 1S6
hamarneh@sfu.ca

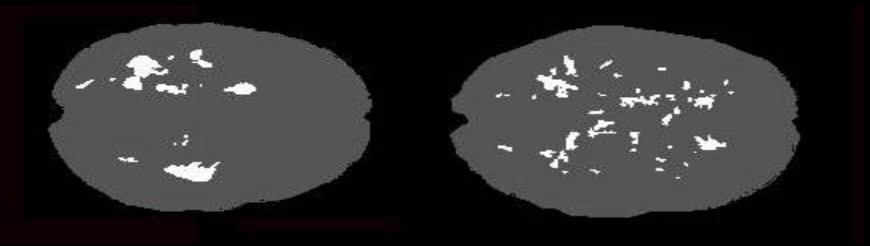

2.2. Lesion dispersion measures

Compactness. Developed by Bribiesca [4] to quantify the connectedness of shapes composed of cubic voxels, compactness is mathematically defined as follows:

$$C = \frac{n - A/6}{n - (\sqrt[3]{n})^2} \tag{1}$$

JOURNAL OF MAGNETIC RESONANCE IMAGING 29:1190–1194 (2009)

Clinical Note

Diminished Visibility of Cerebral Venous Vasculature in Multiple Sclerosis by Susceptibility-Weighted Imaging at 3.0 Tesla

Yulin Ge, MD,[1*] Vahe M. Zohrabian, MD,[1] Etin-Osa Osa, MD,[1] Jian Xu, PhD,[2] Hina Jaggi, RT,[1] Joseph Herbert, MD,[3] E. Mark Haacke, PhD,[4] and Robert I. Grossman, MD[1]

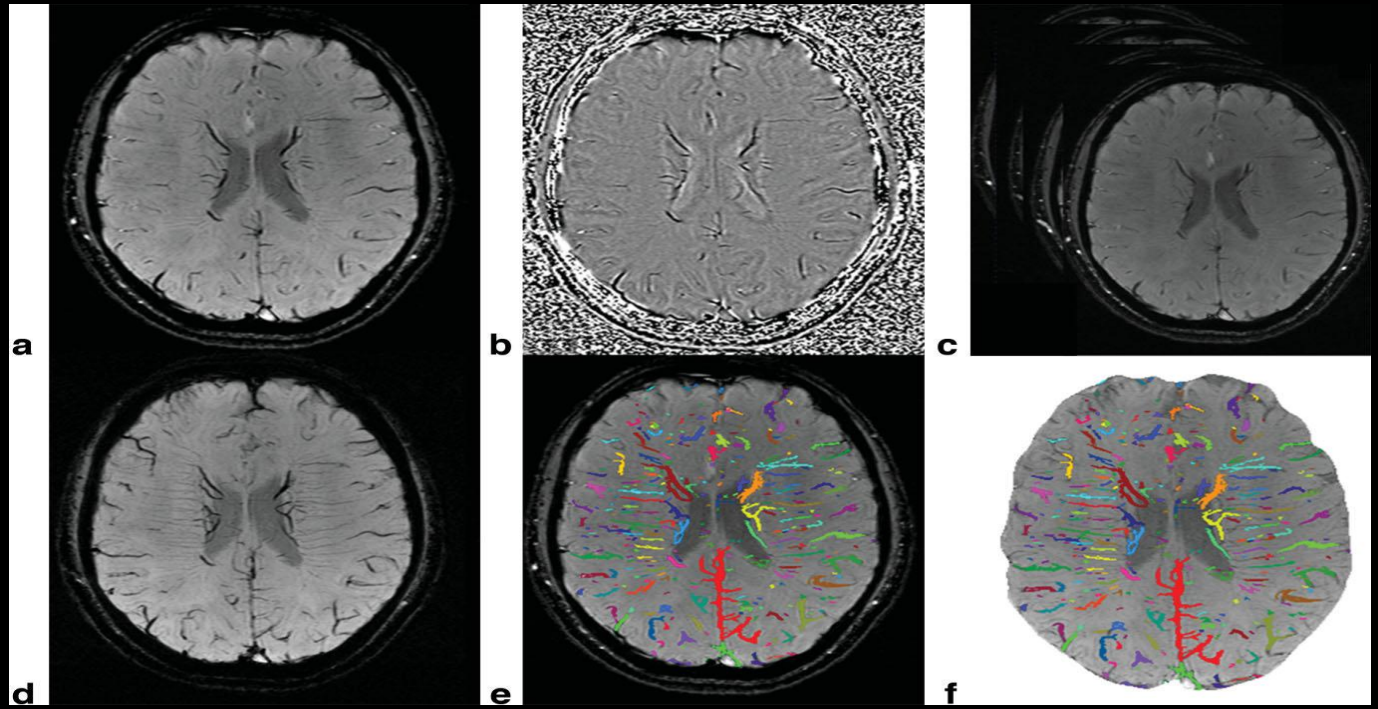

Three-dimensional high resolution venography using susceptibility weighted imaging at 7T

Yulin Ge[1*], Samuel Barnes[2], Samantha Heller[1], Daniel K. Sodickson[1], Lin Tang[1], E. Mark Haacke[2], Jianping Dai[3], Robert I. Grossman[1]

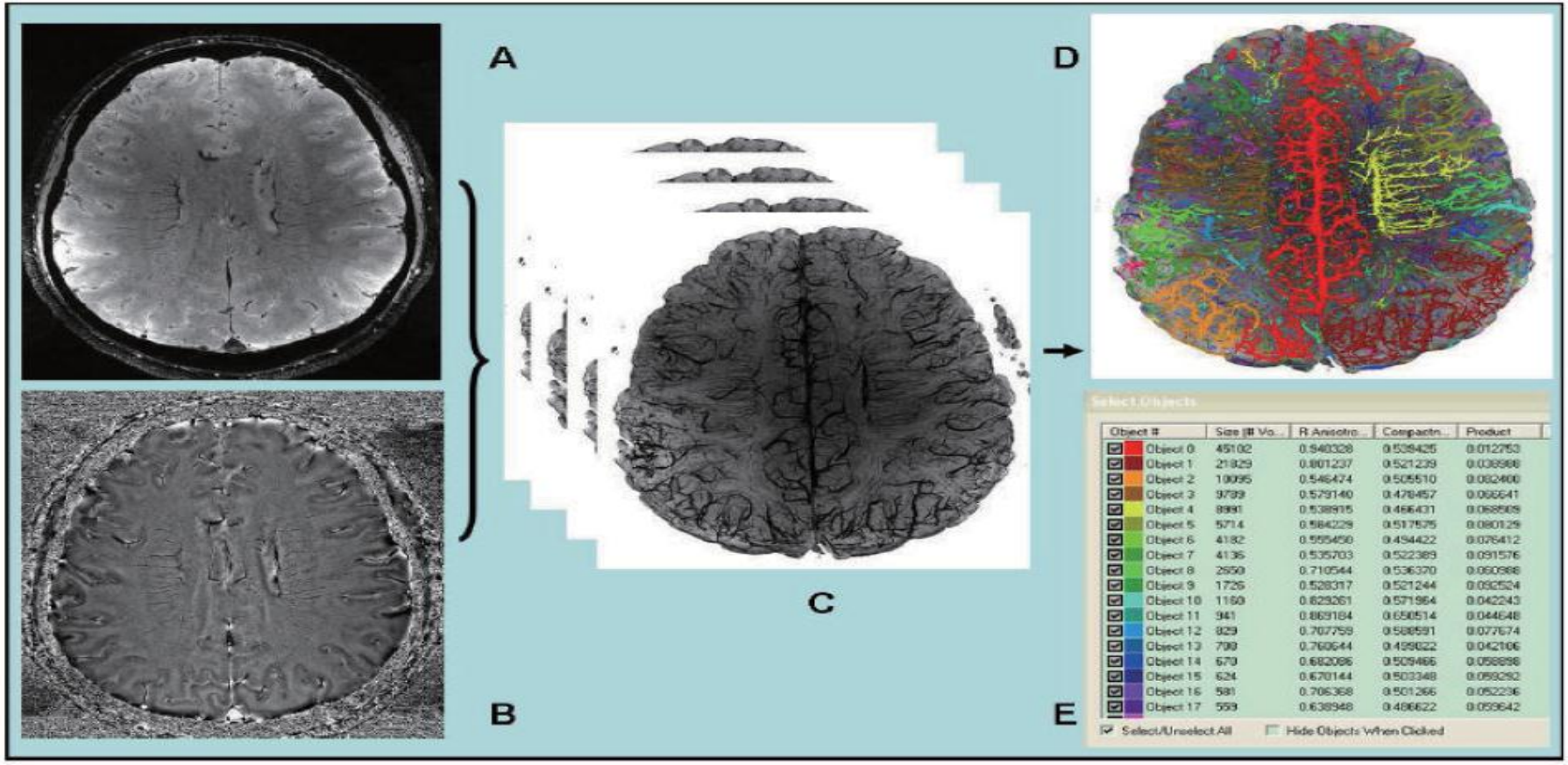

Available online at www.sciencedirect.com
ScienceDirect
Magnetic Resonance Imaging 29 (2011) 844–852
MAGNETIC RESONANCE IMAGING

Semiautomated detection of cerebral microbleeds in magnetic resonance images ☆

Samuel R.S. Barnes[a,b,c,*], E. Mark Haacke[a,b,c,d], Muhammad Ayaz[e], Alexander S. Boikov[c,f], Wolff Kirsch[g], Dan Kido[b]

[a]Department of Biomedical Engineering, Wayne State University, Detroit, MI 48201, USA
[b]Department of Radiology, Loma Linda University Medical Center, Loma Linda, CA 92350, USA
[c]The Magnetic Resonance Imaging Institute for Biomedical Research, Detroit, MI 48202, USA
[d]Department of Radiology, Wayne State University, Detroit, MI 48201, USA
[e]Hemorrhagic Stroke Research Center, Department of Neurology, Massachusetts General Hospital, Harvard Medical School, Boston, MA 02114, USA
[f]Wayne State University School of Medicine, Detroit, MI 48201-1998, USA
[g]Neurosurgery Center for Research, Training and Education, Loma Linda University, Loma Linda, CA 92350, USA

Received 22 October 2010; revised 10 February 2011; accepted 20 February 2011

Compactness is approximately a ratio of surface area to volume, with spheres having the highest theoretical compactness. Cerebral microbleeds, therefore, have a very high compactness and veins have a very low compactness. Since we are dealing with discrete voxels, compactness is calculated by counting adjacent voxel faces:

$$C_d = \frac{A_C - A_{Cmin}}{A_{Cmax} - A_{Cmin}} \quad (3)$$

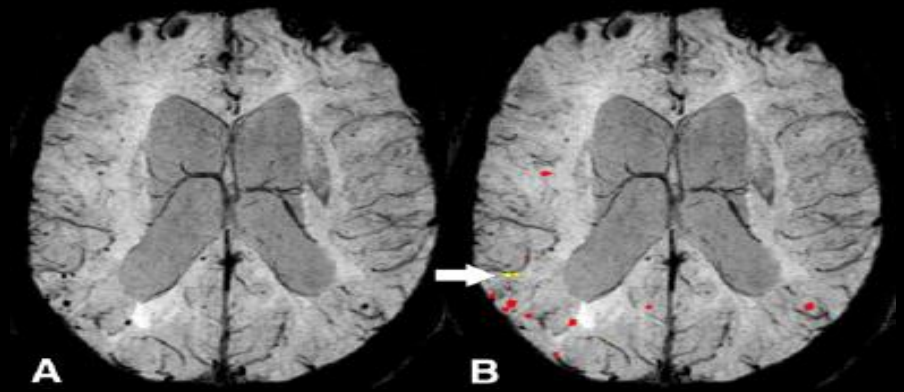

A Voxel-Based Measure of Discrete Compactness for Brain Imaging

E. Bribiesca[1,2], J. R. Jimenez[1], V. Medina[1], R. Valdes[1], O. Yanez[1]
[1]Department of Electrical Engineering, Universidad Autonoma Metropolitana, Iztapalapa, Mexico
[2]In sabbatical leave at [1], Mailing Address: Department of Computer Science, IIMAS, Universidad Nacional Autonoma de Mexico, Apdo. 20-726, Mexico, D.F. 01000 email: ernesto@leibniz.iimas.unam.mx

ELSEVIER

Available online at www.sciencedirect.com
ScienceDirect

Pattern Recognition 41 (2008) 543–554

PATTERN RECOGNITION
THE JOURNAL OF THE PATTERN RECOGNITION SOCIETY
www.elsevier.com/locate/pr

An easy measure of compactness for 2D and 3D shapes

Ernesto Bribiesca*

Departamento de Ciencias de la Computación, Instituto de Investigaciones en Matemáticas Aplicadas y en Sistemas, Universidad Nacional Autónoma de México, Apdo. Postal 20-726, D.F., 01000, México

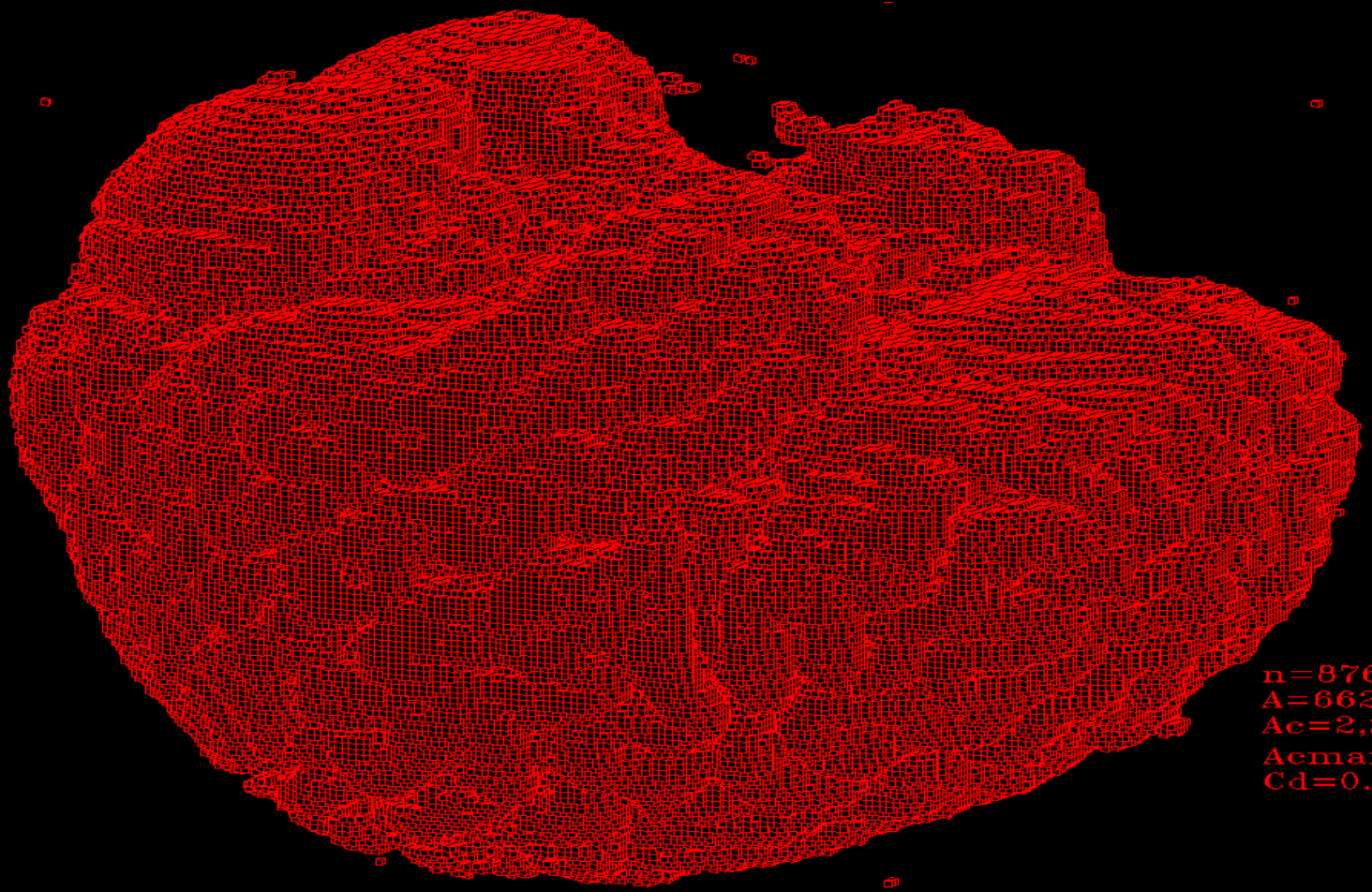
n=876,467 voxels
A=662,672
Ac=2,298,065
Acmax=2,601,927
Cd=0.8238
UAM-UNAM

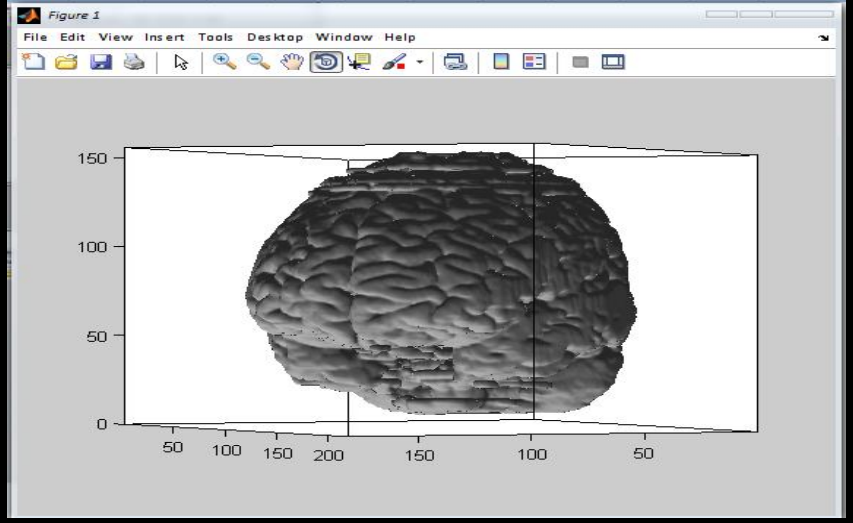
Figure 1
File Edit View Insert Tools Desktop Window Help
150
100
50
0
50 100 150 200 150 100 50

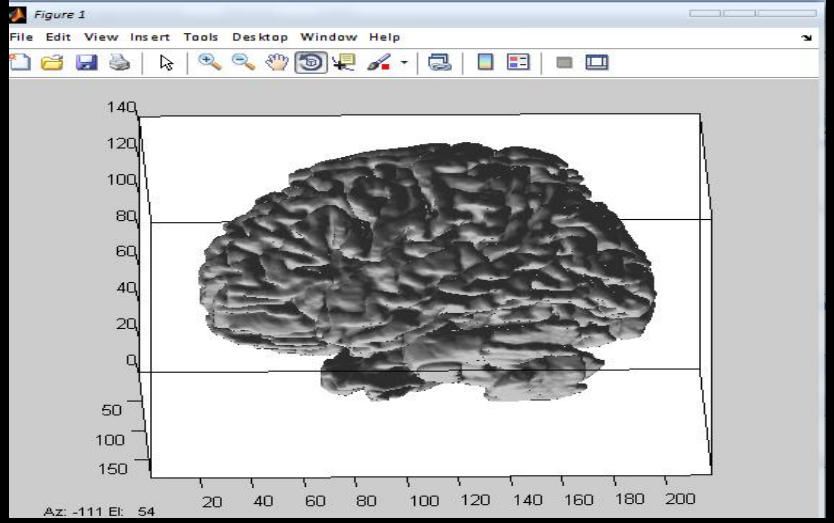
Figure 1
File Edit View Insert Tools Desktop Window Help
140
120
100
80
60
40
20
0
50
100
150
20 40 60 80 100 120 140 160 180 200
Az: -111 El: 54

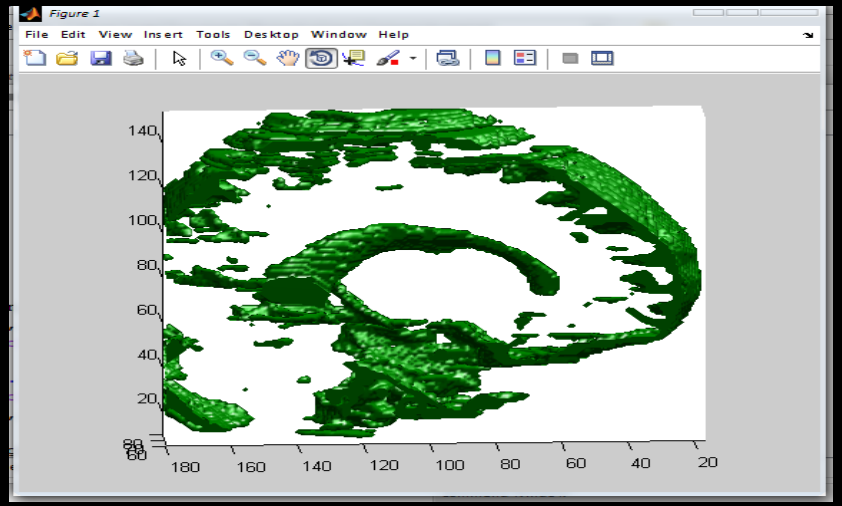
Figure 1
File Edit View Insert Tools Desktop Window Help
140
120
100
80
60
40
20
180 160 140 120 100 80 60 40 20

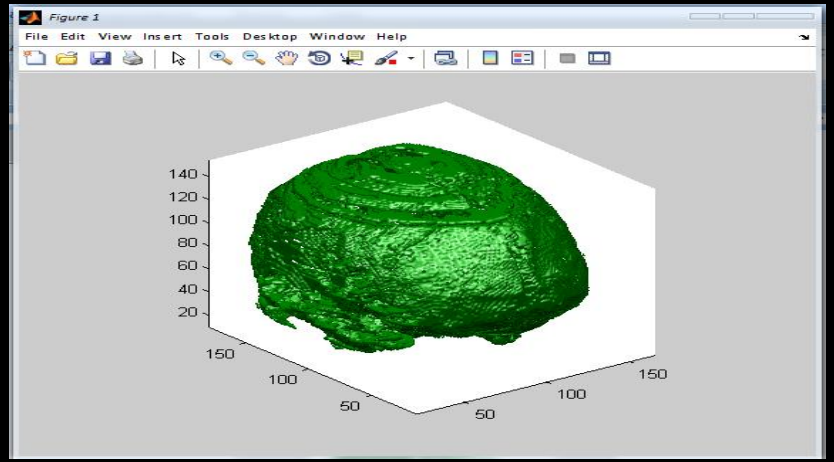
Figure 1
File Edit View Insert Tools Desktop Window Help
140
120
100
80
60
40
20
150
100
50
50
100
150

Resultados preliminares

Dra. Verónica Medina, Jorge Luis Pérez

Estructura	Volumen	Área envolvente	Área de contacto	Compacidad discreta	Componentes conexas	Agujeros	Numero de Euler
Materia gris	944,446	685,600	2,490,538	0.880634163	9	19	-10
Materia blanca	678,695	385,866	1,843,152	0.915662579	9	2	7
L.Cefalorraquídeo	326,677	404,404	777,829	0.805371788	57	2	55

Available online at www.sciencedirect.com
ScienceDirect
Computerized Medical Imaging and Graphics 31 (2007) 428–435
Computerized Medical Imaging and Graphics
www.elsevier.com/locate/compmedimag

Evaluation of the invasion front pattern of squamous cell cervical carcinoma by measuring classical and discrete compactness

Jens Einenkel [a,*], Ulf-Dietrich Braumann [b], Lars-Christian Horn [c], Nadine Pannicke [a], Jens-Peer Kuska [b], Alexander Schütz [c], Bettina Hentschel [d], Michael Höckel [a]

[a] *Department of Obstetrics and Gynecology, Leipzig University, Germany*
[b] *Interdisciplinary Centre for Bioinformatics & Translational Centre for Regenerative Medicine, Leipzig University, Germany*
[c] *Institute of Pathology, Leipzig University, Germany*
[d] *Institute of Medical Informatics, Statistics and Epidemiology, Leipzig University, Germany*

Received 19 November 2005; received in revised form 20 March 2007; accepted 26 March 2007

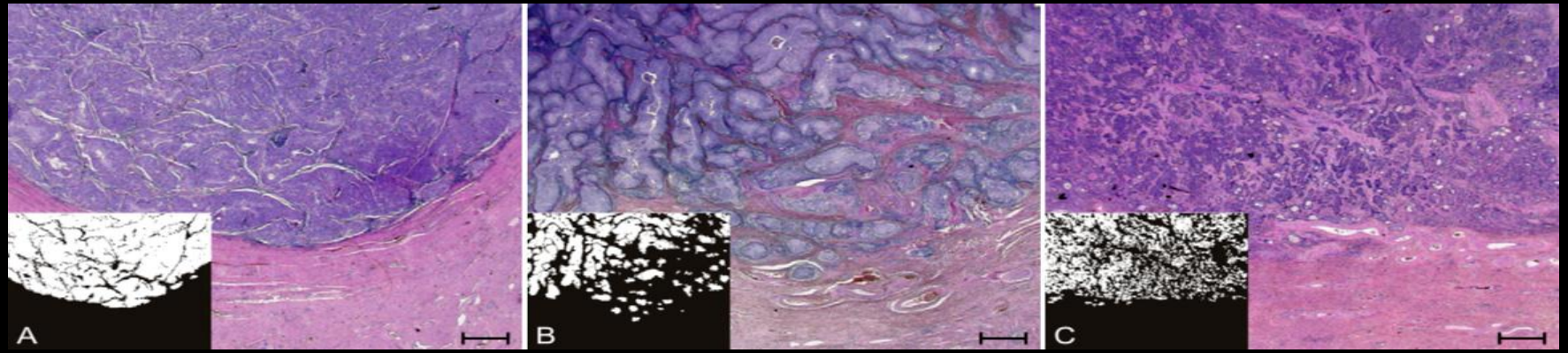

Contact Knots

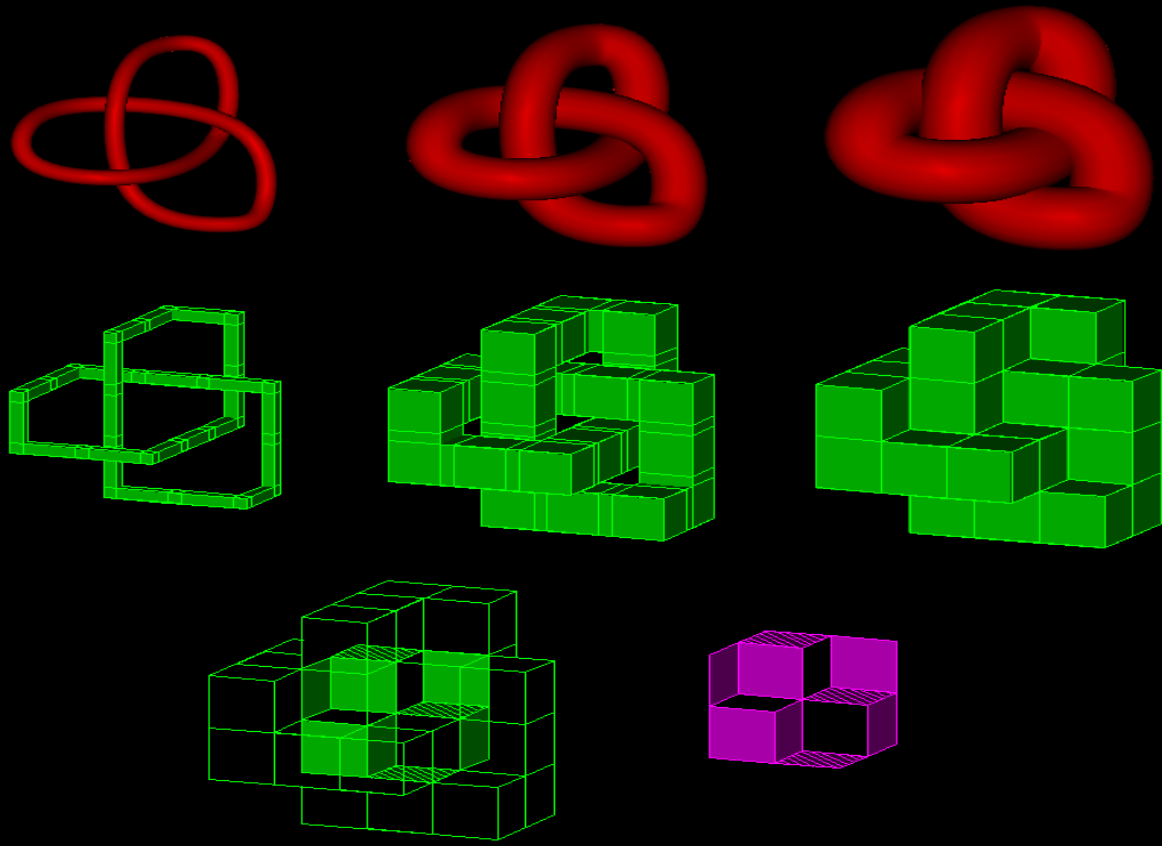

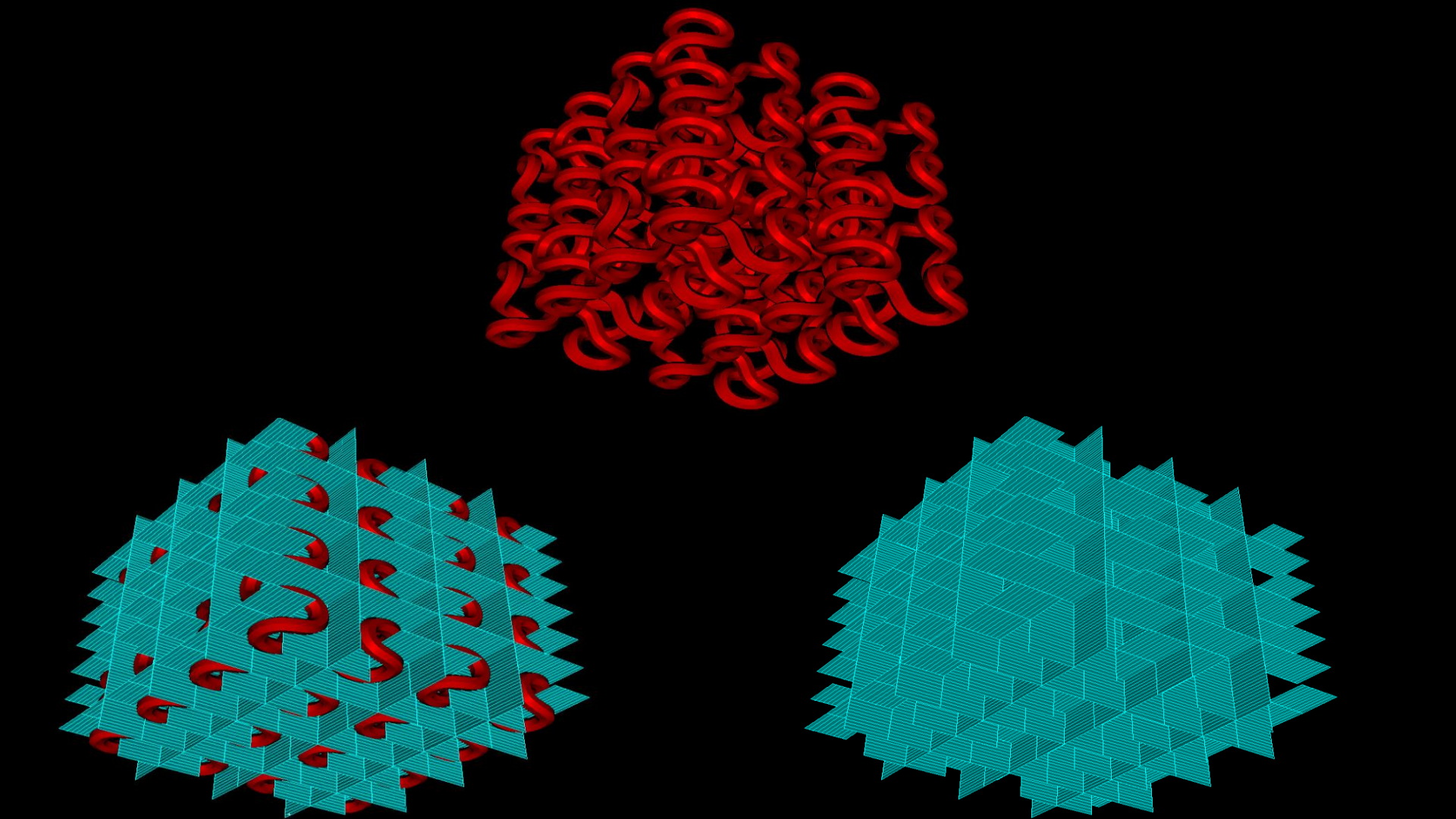

(12) INTERNATIONAL APPLICATION PUBLISHED UNDER THE PATENT COOPERATION TREATY (PCT)

(19) World Intellectual Property Organization
International Bureau

WO 2006/044988 A1

(54) Title: SYSTEM AND METHOD FOR CHARACTERIZING 3-DIMENSIONAL SHAPE BY [illegible] DESCRIPTORS

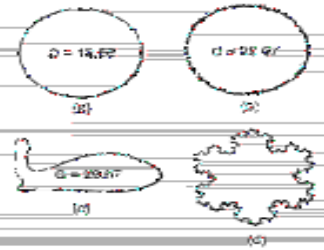

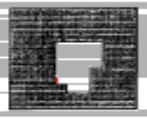

Complex segmented medical digital scan

Contents lists available at ScienceDirect

Computers and Mathematics with Applications

journal homepage: www.elsevier.com/locate/camwa

Computation of the Euler number using the contact perimeter

Ernesto Bribiesca *

Departamento de Ciencias de la Computación, Instituto de Investigaciones en Matemáticas Aplicadas y en Sistemas, Universidad Nacional Autónoma de México, Apdo. 20-726, México, D.F., 01000, Mexico

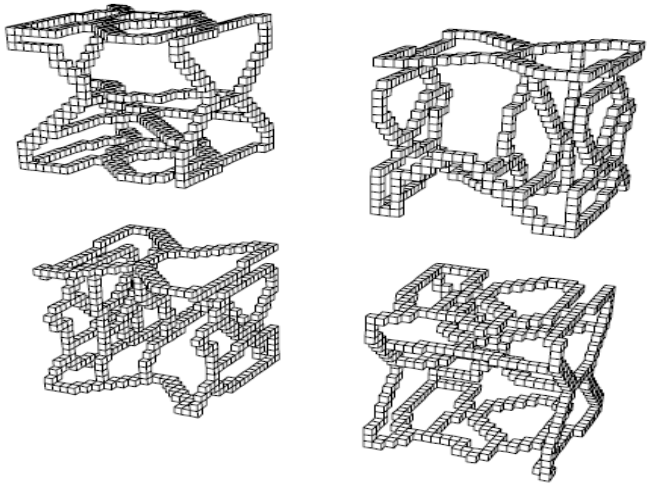

Euler

$$F + V - E = 2$$

Contact Perimeter

$$H = \frac{2P_c - P}{4} + 1$$